CHEMICAL ENGINEERING TRANSACTIONS
VOL. 94, 2022
A publication of AIDIC
The Italian Association of Chemical Engineering
Online at www.cetjournal.it
Guest Editors: Petar S. Varbanov, Yee Van Fan, Jiří J. Klemeš, Sandro Nižetić

ISBN 978-88-95608-93-8; **ISSN** 2283-9216
DOI: 10.3303/CET2294097

The Effect of the Presence of Mist in the Proposed Sonophotocatalytic Wastewater Treatment Process

Shoma Kato, Yuka Sakai, Yuki Sato, Yasuki Kansha*

Organization for Programs on Environmental Sciences, Graduate School of Arts and Sciences, The University of Tokyo, 3-8-1 Komaba, Meguro-ku, Tokyo 153-8902 JAPAN
kansha@global.c.u-tokyo.ac.jp

Advanced oxidation processes (AOPs) involve the generation of highly reactive hydroxyl radicals and can efficiently treat refractory organic compounds in wastewater. Photocatalytic AOPs use photocatalysts that utilize light. The performance of photocatalytic reactions can be limited by the surface area of the catalyst and mass transfer of the contaminants. Sonophotocatalytic processes that involve the combination of sonocatalysis and photocatalysis have been studied for improved pollutant removal. To further improve the process, a sonophotocatalytic process that utilizes the mist particles that are generated via ultrasound is proposed. Some of the features of the mist include its increased surface area and shorter light penetration distance. Using TiO_2 as the photocatalyst and phenol as the representative organic contaminant, the effect of the mist particles on the sonophotocatalytic process was assessed. The results of the experiment demonstrated that the generation of mist particles increased the apparent rate of the removal of phenol by 31.3 %. Additionally, the properties of the TiO_2 catalyst after ultrasound and UV irradiation were investigated. In the future designs of sonophotocatalytic processes, the mist particles may be utilized to improve the removal of refractory organics.

1. Introduction

Water scarcity from global population and economic growth is an urgent issue (Boretti and Rosa, 2019). Technologies such as desalination and the reuse of treated water may reduce water scarcity (van Vliet et al., 2021). The demanded water quality and the generated wastewater depend on the sector (i.e. municipal, industrial, and agricultural) and the usage of the water within the sector. This study focuses on the treatment of industrial wastewater since it contains organic compounds that are resistant to conventional biological treatment (Oller et al., 2011). To treat those organic compounds, advanced oxidation processes (AOPs) have been studied and implemented. AOPs are processes that involve the generation of highly reactive hydroxyl radicals (Glaze et al., 1987). Hydroxyl radicals can be generated by chemical, photochemical, Sonochemical, and electrochemical reactions (Oturan and Aaron, 2014). Photocatalytic AOPs use photocatalysts for the generation of hydroxyl radicals. TiO_2 is a catalyst that is used often used as a photocatalyst since it is chemically stable, durable, low-cost, and non-toxic (Nakata and Fujishima, 2012). The performance of photocatalysts to degrade organic pollutants in water is limited by mass transfer and the amount of UV irradiation on the catalyst surface. Hybrid processes such as the photocatalytic circulating-bed biofilm reactor which involve photocatalytic and biological degradation (Marsolek et al., 2008), and photocatalytic membranes that involve photocatalytic reactions and membrane separation process (Zhang et al., 2006). The sonophotocatalytic process involves the simultaneous irradiation of ultrasound (US) and UV in the presence of a catalyst. Some advantages of the sonophotocatalytic process include cleaning of the catalyst surface, improved mass transfer (van de Moortel et al., 2020), and the generation of free radicals by sonolysis and sonocatalysis (Kakavandi et al., 2019).
To further improve pollutant removal with the sonophotocatalytic process, the utilization of atomization mist generated by US irradiation has been considered. Rahimi et al. (2016) investigated the sonophotocatalytic removal of ammonia with atomization mist produced by high-frequency US of 1.7 MHz. Itoh and Kojima (2019) evaluated the synergistic effect of the sonophotocatalysis with atomization mist by US irradiation of 500 kHz on the oxidation of potassium iodide. Li et al. (2020) studied the degradation of 2,4,6-trichlorophenol with photocatalysts and atomization mist, and the comparison of the sonophotocatalysis with and without the mist

Paper Received: 15 April 2022; Revised: 06 May 2022; Accepted: 06 May 2022
Please cite this article as: Kato S., Sakai Y., Sato Y., Kansha Y., 2022, The Effect of the Presence of Mist in the Proposed Sonophotocatalytic Wastewater Treatment Process, Chemical Engineering Transactions, 94, 583-588 DOI:10.3303/CET2294097

was not made. Ono et al. (2020) studied the degradation of aldehydes using US atomization and UV irradiation without the use of a photocatalyst. The authors have investigated the sonophotocatalytic removal of phenol with atomization mist and compared its performance with photocatalysis (Kato et al., 2021). To the best of knowledge, the comparison of the sonophotocatalytic process with and without US atomization mist has not been made, and the effect of US and UV irradiation on the TiO_2 photocatalyst has not been studied.
In this study, the improvement of phenol removal in the sonophotocatalytic process by the presence of US atomization mist was investigated. Additionally, the change in the crystal composition, thermal properties, and UV-vis absorbance characteristics of the TiO_2 catalyst before and after US and UV irradiation was analyzed. The amount of mist generation by the US unit was measured to assess the potential to utilize mist.

2. Experimental

2.1 Chemicals

Phenol (99 %, Fujifilm Wako Pure Chemical Corporation) was used as the representative organic compound and Aeroxide P25 TiO_2 (Brunauer-Emmett-Teller specific surface area = 53 m^2/g, Nippon Aerosil Co., Ltd.) was selected as the photocatalysts in the experiments. These reagents were used without further purification or treatment. Ultrapure water (resistivity = 18.2 MΩ·cm) generated using an ultrapure water generation unit (Simplicity UV, Merck) was used as the dilutant.

2.2 Comparison of the sonophotocatalytic process with and without mist generation

The sonophotocatalytic reactor that was used is described in earlier studies by the authors (Kato et al., 2021). The UV lamp (4 W, LUV-4, AS ONE Corporation) has a main wavelength of 365 nm. The frequency and power of the US atomization unit (IM1-24, Seiko Giken Inc.) are 1.6-1.7 MHz and about 21.6 W respectively. The vessel was filled with 300 mL of 50 mg/L phenol solution with a TiO_2 dosage of 1 g/L. For the adsorption of phenol onto the catalyst, the solution after adding TiO_2 was agitated with a magnetic stirrer at 500 rpm for 1 min, sonicated in a US bath for 30 s, and agitated again for 1 h. To assess the improvement by the mist generation, experiments were conducted with the reactor under the condition that mist is generated and the condition that no mist is generated. For the case when the mist was not generated, the vessel was filled with glass beads (diameter of about 1.24 cm) which have a total volume of 131 cm^3.
3 mL samples were taken with a syringe and filtered using polyethersulfone (PES) membrane syringe filters (pore size = 0.1 µm). The absorbance of the sample was measured using a UV-vis spectrophotometer (UV-2600i, Shimadzu Corporation). Phenol removal was calculated by the following equation (Kato et al., 2021):

$$Phenol\ removal\ (\%) = \frac{C_0 - C_t}{C_0} \times 100 \quad (1)$$

where C_0 and C_t are the phenol concentration (mg/L) initially and at time t respectively.

2.3 Measurement of the amount of mist generation

The amount of the mist was measured using the setup shown in Figure 1. The length, width, and height of the vessel used are 17.3 cm, 17.3 cm, and 15.3 cm. The US atomization unit was placed inside the vessel. Then, the vessel was filled with water so that the height of the liquid was 5.5 cm which is the height used in the earlier experiments (Kato et al., 2021). The vessel was placed on top of a scale inside of a fume hood. Air at room temperature was blown with a compressor on the generated mist to remove the mist from the vessel. The US atomization unit was turned on for 1 min and turned off to observe the mass difference by using the reading from the scale.

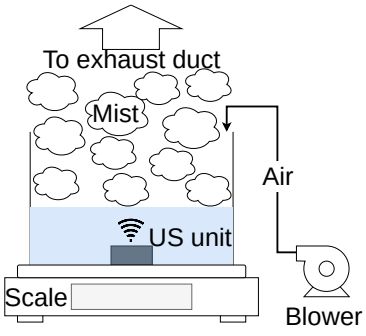

Figure 1: The experimental setup used to measure the mist generation amount by the US atomization unit

2.4 Characterization of the catalyst

The TiO_2 catalyst before and after US and UV irradiation were analyzed. The TiO_2 catalyst was filtered from the mixture by filtration with a filter paper and drying. The crystal properties of the catalyst were observed using an X-ray diffraction (XRD) analyzer (MiniFlex600, Rigaku Corporation) with a monochromatic Cu$K\alpha$ radiation source. The UV-vis spectrum of the TiO_2 catalyst was measured using a UV-vis spectrophotometer equipped with an integrating sphere (ISR-2600PLUS, Shimadzu Corporation) to quantify the change in the absorbance wavelength of the catalyst after US and UV irradiation. $BaSO_4$ (NACALAI TESQUE, INC.) was used as the reference for the baseline. The thermal behavior of the catalyst was observed using a thermogravimetric and differential thermal analyzer (TG-DTA8122, Rigaku Corporation) with air from 25 to 1,000 °C with a heating rate of 5.0 °C/min.

3. Results and discussion

3.1 Amount of mist generation

In the current experimental setup for sonophotocatalytic degradation, the mist is contained in the space above the surface of the liquid bulk in the beaker. The amount of mist is saturated since the mist clump together and fall into the liquid bulk again. Increasing the quantity of mist is expected to increase pollutant removal since it can improve photocatalytic degradation (Li et al., 2020). The mist generation was measured (Figure 2) to evaluate the potential amount of mist that can be utilized for the photocatalytic reaction. The average amount of mist generated was 4.1 g/min in the 10 trials. To improve the process in the future, the mist may be utilized more by increasing the quantity of the mist by optimizing the liquid level in the vessel, by increasing the floating duration of the mist by using a larger vessel, and by transporting the mist to another vessel.

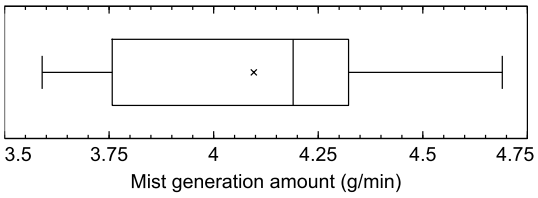

Figure 2: The amount of mist generated from the US atomization unit

3.2 Sonophotocatalysis with mist versus without mist

Figure 3 shows the comparison of the sonophotocatalytic process with and without mist generation. After 180 min, the phenol removal with mist and without mist was 14.3 % and 11.1 % respectively. The apparent rate of phenol removal can be calculated by assuming a Langmuir-Hinshelwood pseudo-first-order model for low concentrations of phenol (Darabdhara et al., 2016) with the following equation:

$$\ln(C_0/C_t) = k_a t \tag{2}$$

where k_a is the apparent rate constant (min^{-1}) and C_0 and C_t are the phenol concentrations (mg/L) initially and at time t (min). The apparent rate constant k_a is calculated by linear regression using Eq(2).

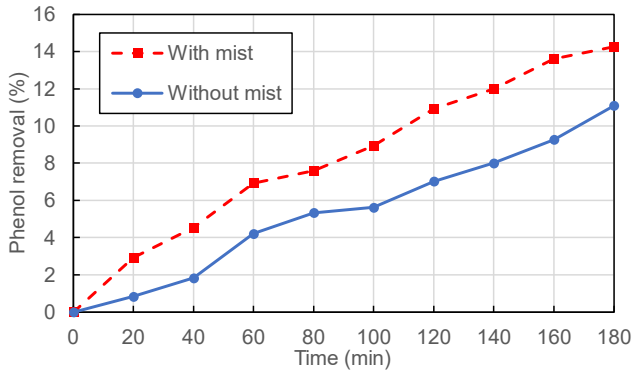

Figure 3: Comparison of the sonophotocatalytic process with and without mist generation

For sonophotocatalysis with no mist and with mist, the apparent rate constant k_a was 6.36×10^4 min^{-1} (R^2 = 0.987) and 8.35×10^4 min^{-1} (R^2 = 0.986) respectively. The apparent rate increases by 31.3 % with the presence of mist under the current experimental conditions.
The presence of the US atomization mist may improve the reaction by the presence of TiO_2 in the mist (Kato et al., 2021) which allows photocatalytic reactions to occur with the mist (Rahimi et al., 2016). The advantages of the mist include improved UV utilization due to the larger surface area of the mist (Itoh and Kojima, 2019), the shorter distance of light penetration, and improved mass transfer. With higher TiO_2 dosages, the UV intensity decreases rapidly as the distance from the light source increases (van de Moortel et al., 2020). With the small size of the atomization mist, UV light can be transmitted and utilized by the catalyst more easily.

3.3 Properties of the catalyst before and after US and UV irradiation

To investigate the effect of US and UV irradiation on the TiO_2 catalyst, the XRD pattern was analyzed. The XRD pattern of the anatase and rutile phase of the TiO_2 was obtained from the Crystallography Open Database (COD) which is an open-access database that provides structural data (Gražulis et al., 2009). Figure 4 shows the XRD pattern of the TiO_2 P25 catalyst before and after the US and UV irradiation from the experiments where the anatase (COD ID: 5000223, (Horn et al., 1972)) and rutile (COD ID: 9015662, (Howard et al., 1991)) diffraction peaks are shown. The position of the peaks remains the same before and after US and UV irradiation, indicating that anatase and rutile Quantitative analysis of the crystal structure of the TiO_2 catalyst was performed using SmartLab Studio II (Rigaku Corporation) software with the reference intensity ratio (RIR) method. Before US and UV irradiation, the weight fraction of the anatase and rutile phases were 88.20±0.19 % and 11.80±0.19 % respectively. After US and UV irradiation, the weight fraction of the anatase and rutile phases were 88.11±0.09 % and 11.89±0.19 % respectively. Thus, there was little to no change in the weight fraction of the crystal structure indicating that the anatase and rutile crystals of the TiO_2 P25 catalyst are stable under US and UV irradiation.

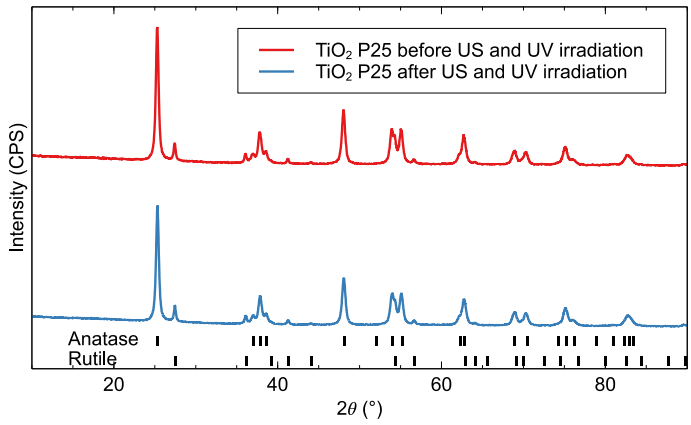

Figure 4: XRD pattern before and after US and UV irradiation

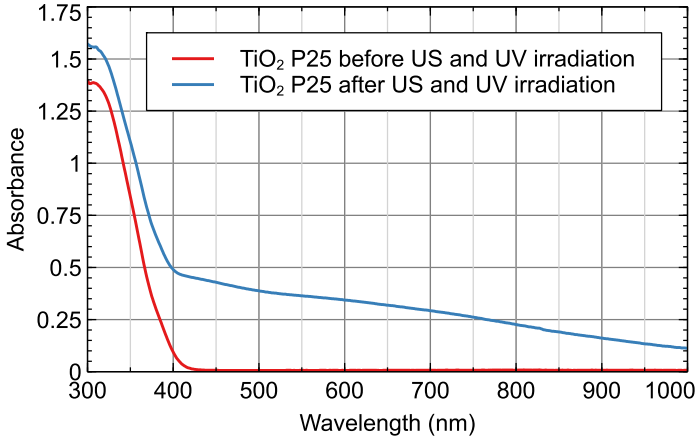

Figure 5: UV-vis spectrum of the TiO_2 P25 before and after US and UV irradiation

The filtered and dried catalyst after US and UV irradiation appeared to be a gray color compared to the initial white color of the catalyst. The UV-vis spectrum of the TiO_2 P25 catalyst is shown in Figure 5. The TiO_2 catalyst after US and UV irradiation absorbs light in the visible region and the UV region. The reason for the gray color could be due to the formation of oxygen vacancies from Ti^{3+} (Bi et al., 2021). This phenomenon can also occur with the addition of hydrogen via ultrasonication (Fan et al., 2015).
The TG-DTA profile of the TiO_2 catalyst is shown in Figure 6 for the analysis of the thermal properties of the catalyst before and after US and UV irradiation. In both cases, the mass loss is observed from room temperature to around 150 °C due to the evaporation of water adsorbed by the catalyst. There is also a mass loss for both from 150 °C to about 500 °C due to the loss of the strongly bound water and hydroxyls (Nagaveni et al., 2004). Additionally, the crystalline phase transition from anatase to rutile occurs in both cases starting at around 600 °C and peaking at around 840 °C. For the catalyst after US and UV irradiation, the mass increases very gradually from around 500 °C. This is likely due to the addition of oxygen to the oxygen vacancies of the TiO_2 catalyst formed after US and UV irradiation.

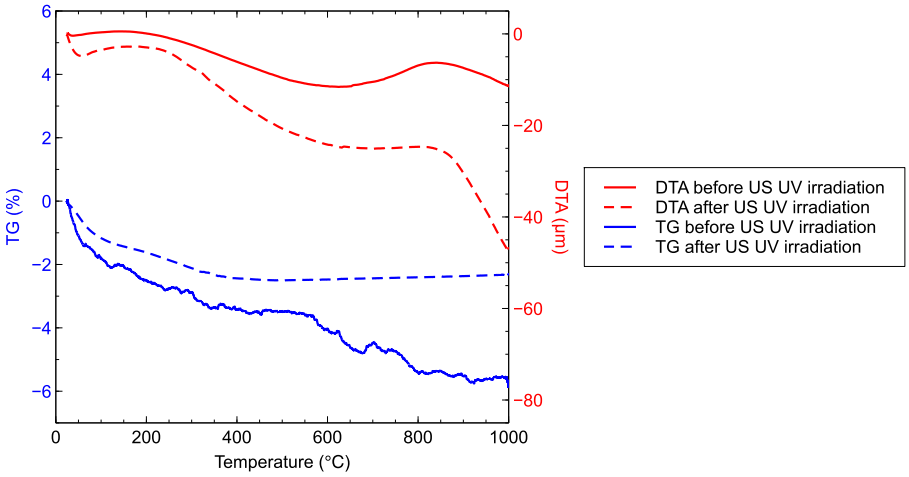

Figure 6: TG-DTA of the TiO_2 catalyst before and after US and UV irradiation

The results of the XRD analysis and the UV-vis absorption spectrum suggest that the TiO_2 catalyst crystal composition is stable under US and UV irradiation, but the absorbance of visible and UV light increases. From the thermal analysis, the crystalline phase transition was observed due to the high temperature. US irradiation can cause high local temperatures and pressure due to acoustic cavitation (Suslick, 1990). The XRD and thermal analysis results suggest that the TiO_2 catalyst crystal composition is stable even with cavitation.

4. Conclusions

In this study, the removal of phenol with the sonophotocatalysis with and without US atomization mist was compared. The results support that the proposed process with the presence of mist is effective and improves the sonophotocatalytic treatment of organic pollutants. With the presence of mist, the apparent rate increased by 31.3 %. The mist can be utilized further since 4.1 g/min on average can be generated by the US atomization unit. The TiO_2 catalyst was analyzed before and after US and UV irradiation. While high temperature can cause crystalline phase transition from the TG-DTA results, the X-ray diffraction results indicate little to no change in the crystal structure composition of the catalyst despite cavitation from US irradiation. The UV-vis absorption spectra show that UV and visible light absorption of the catalyst increases after US and UV irradiation.

Acknowledgments

This work was supported by Japan Science and Technology Agency (JST) SICORP Grant Number JPMJSC18H5 and the Japan Prize Foundation.

References

Bi X., Du G., Kalam A., Sun D., Yu Y., Su Q., Xu B., Al-Sehemi A.G., 2021, Tuning oxygen vacancy content in TiO_2 nanoparticles to enhance the photocatalytic performance, Chemical Engineering Science, 234, 116440.

Boretti A., Rosa L., 2019, Reassessing the projections of the World Water Development Report, Npj Clean Water, 2 (1), 1–6.

Darabdhara G., Boruah P.K., Borthakur P., Hussain N., Das M.R., Ahamad T., Alshehri S.M., Malgras V., Wu K.C.W., Yamauchi Y., 2016, Reduced graphene oxide nanosheets decorated with Au-Pd bimetallic alloy nanoparticles towards efficient photocatalytic degradation of phenolic compounds in water, Nanoscale, 8 (15), 8276–8287.

Fan C., Chen C., Wang J., Fu X., Ren Z., Qian G., Wang Z., 2015, Black Hydroxylated Titanium Dioxide Prepared via Ultrasonication with Enhanced Photocatalytic Activity, Scientific Reports, 5 (1), 1–10.

Glaze W.H., Kang J.W., Chapin D.H., 1987, The chemistry of water treatment processes involving ozone, hydrogen peroxide and ultraviolet radiation, Ozone: Science & Engineering, 9 (4), 335–352.

Gražulis S., Chateigner D., Downs R.T., Yokochi A.F.T., Quirós M., Lutterotti L., Manakova E., Butkus J., Moeck P., Le Bail A., 2009, Crystallography Open Database – an open-access collection of crystal structures, Journal of Applied Crystallography, 42 (4), 726–729.

Horn M., Schwerdtfeger C.F., Meagher E.P., 1972, Refinement of the structure of anatase at several temperatures, Zeitschrift Fur Kristallographie - New Crystal Structures, 136 (3–4), 273–281.

Howard C.J., Sabine T.M., Dickson F., 1991, Structural and thermal parameters for rutile and anatase, Acta Crystallographica Section B Structural Science, 47 (4), 462–468.

Itoh T., Kojima Y., 2019, Synergistic effects of ultrasound and ultraviolet light irradiation on oxidation reaction using photocatalyst, Journal of Chemical Engineering of Japan, 52 (12), 877–881.

Jiang X., Zhang Y., Jiang J., Rong Y., Wang Y., Wu Y., Pan C., 2012, Characterization of Oxygen Vacancy Associates within Hydrogenated TiO_2 : A Positron Annihilation Study, The Journal of Physical Chemistry C, 116 (42), 22619–22624.

Kakavandi B., Bahari N., Rezaei Kalantary R., Dehghani Fard E., 2019, Enhanced sono-photocatalysis of tetracycline antibiotic using TiO_2 decorated on magnetic activated carbon (MAC@T) coupled with US and UV: A new hybrid system, Ultrasonics Sonochemistry, 55, 75–85.

Kato S., Sakai Y., Sato Y., Kansha Y., 2021, The Effect of High-frequency Ultrasound on the Photocatalytic Decomposition of Organic Compounds in Water, Chemical Engineering Transactions, 88, 379–384.

Li H., Chang X., Zhang Y., Zhang S., Dai Y., Yin L., 2020, Degradation of 2,4,6-trichlorphenol by producing hydrogen using ultrasonic mist generated from photocatalysts suspension, Emerging Contaminants, 6, 155–161.

Marsolek M.D., Torres C.I., Hausner M., Rittmann B.E., 2008, Intimate coupling of photocatalysis and biodegradation in a photocatalytic circulating-bed biofilm reactor, Biotechnology and Bioengineering, 101 (1), 83–92.

Nagaveni K., Sivalingam G., Hegde M.S., Madras G., 2004, Solar photocatalytic degradation of dyes: high activity of combustion synthesized nano TiO_2, Applied Catalysis B: Environmental, 48 (2), 83–93.

Nakata K., Fujishima A., 2012, TiO_2 photocatalysis: Design and applications, Journal of Photochemistry and Photobiology C: Photochemistry Reviews, 13 (3), 169–189.

Oller I., Malato S., Sánchez-Pérez J.A., 2011, Combination of Advanced Oxidation Processes and biological treatments for wastewater decontamination—A review, Science of The Total Environment, 409 (20), 4141–4166.

Ono Y., Sekiguchi K., Sankoda K., Nii S., Namiki N., 2020, Improved ultrasonic degradation of hydrophilic and hydrophobic aldehydes in water by combined use of atomization and UV irradiation onto the mist surface, Ultrasonics Sonochemistry, 60, 104766.

Oturan M.A., Aaron J.-J., 2014, Advanced Oxidation Processes in Water/Wastewater Treatment: Principles and Applications. A Review, Critical Reviews in Environmental Science and Technology, 44 (23), 2577–2641.

Rahimi M., Moradi N., Faryadi M., Safari S., 2016, Removal of ammonia by high-frequency ultrasound wave (1.7 MHz) combined with TiO_2 photocatalyst under UV radiation, Desalination and Water Treatment, 57 (34), 15999–16007.

Suslick K.S., 1990, Sonochemistry, Science, 247 (4949), 1439–1445.

van de Moortel W., Kamali M., Sniegowski K., Braeken L., Degrève J., Luyten J., Dewil R., 2020, How Photocatalyst Dosage and Ultrasound Application Influence the Photocatalytic Degradation Rate of Phenol in Water: Elucidating the Mechanisms Behind, Water, 12 (6), 1672.

van Vliet M.T.H., Jones E.R., Flörke M., Franssen W.H.P., Hanasaki N., Wada Y., Yearsley J.R., 2021, Global water scarcity including surface water quality and expansions of clean water technologies, Environmental Research Letters, 16 (2), 024020.

Zhang H., Quan X., Chen S., Zhao H., Zhao Y., 2006, Fabrication of photocatalytic membrane and evaluation its efficiency in removal of organic pollutants from water, Separation and Purification Technology, 50 (2), 147–155.